McCoy, S. J. and Kamenos, N. A. (2018) Coralline algal skeletal mineralogy affects grazer impacts. *Global Change Biology*, 24(10), pp. 4775-4783. (doi:10.1111/gcb.14370)

Coralline algal skeletal mineralogy affects grazer impacts

Sophie J. McCoy[1*], Nicholas A. Kamenos[2]

[1] Department of Biological Science, Florida State University, Tallahassee, FL 32306-4295

[2] School of Geographical and Earth Science, University of Glasgow, Glasgow, G12 8QQ, Scotland

[*] Corresponding author, mccoy@bio.fsu.edu

Abstract

In macroalgal-dominated systems, herbivory is a major driver in controlling ecosystem structure. However, the role of altered plant-herbivore interactions and effects of changes to trophic control under global change is poorly understood. This is because both macroalgae and grazers themselves may be affected by global change, making changes in plant-herbivore interactions hard to predict. Coralline algae lay down a calcium carbonate skeleton, which serves as protection from grazing and is preserved in archival samples. Here, we compare grazing damage and intensity to coralline algae *in situ* over 4 decades characterized by changing seawater acidity. While grazing intensity, herbivore abundance and identity remained constant over time, grazing wound width increased together with Mg content of the skeleton and variability in its mineral organization. In one species, decreases in skeletal organization were found concurrent with deeper skeletal damage by grazers over time since the 1980s. Thus, in a future characterized by acidification, we suggest coralline algae may be more prone to grazing damage, mediated by effects of variability between individuals and species.

Introduction

Recent advances in climate change ecology have focused on traits that influence species interactions. In macroalgal-dominated systems, much of this research has centered on herbivory and the scope for altered plant-herbivore interactions and effects of changes to trophic control (Connell & Russell, 2010; Falkenberg *et al.*, 2013; Russell *et al.*, 2013; McCoy & Pfister, 2014; Vergés *et al.*, 2014; Ghedini *et al.*, 2015; McCoy *et al.*, 2016). Similarly, coralline algae stand to be affected by such community processes, yet are also vulnerable as calcifiers amongst macroalgae (McCoy & Kamenos, 2015). Coralline algal resistance to grazers is largely

dependent on thallus thickness (Paine, 1984; Steneck *et al.*, 1991) and morphology (Steneck, 1982). These skeletal morphological traits may be at risk from ocean acidification (McCoy & Ragazzola, 2014), including effects on external and internal skeletal structure metrics. Further, the rate of environmental change (Kamenos *et al.*, 2013) as well as the duration of stress (Ragazzola *et al.*, 2012; 2013) have been shown to affect the magnitude of skeletal impacts in this group.

Previous examination of field specimens from the Northeast Pacific provide evidence for morphology-dependent responses of crustose coralline algal skeletons to ongoing *in situ* ocean acidification between the 1980s and 2010s. The thicker species *Pseudolithophyllum muricatum* and *Lithophyllum impressum* have thinned over time, but have preserved their internal skeletal density (McCoy, 2013; McCoy & Ragazzola, 2014). Conversely, thinner species including *Pseudolithophyllum whidbeyense* have not changed in thickness, but have reduced internal skeletal density (McCoy & Ragazzola, 2014). Together, these results suggest an energetic tradeoff under acidification stress, affecting the quantity of skeletal material laid down. It is therefore likely that changes to the quality of skeletal material, identified by changes in skeletal chemistry, have also occurred over this 30-year span. Both reduced thallus thickness and the potential for reduced quality of skeletal material will have effects on coralline algal traits relevant to competitive or trophic interactions.

Such ecosystem studies are conducted *in situ*, within ecological context, and thus sub-lethal skeletal responses of coralline algae to ocean acidification may be mediated by grazing intensity and damage, or affect the extent to which they are damaged by grazing. Crustose coralline algae

from Mediterranean CO_2 vents (*Lithophyllum, Titanoderma* and *Phymatolithon* spp.) (Kamenos *et al.*, 2016) and temperate laboratory studies (Pauly *et al.*, 2015) (*Lithothamnion glaciale*) provide evidence that they are able to buffer against changes in water pCO_2, preserving their Mg concentrations until extreme (pH <7.4) pCO_2 conditions are encountered demonstrating and absence of sub-lethal skeletal trade-offs in low pH. This is possible because of coralline algal skeletal mineralogy, a high-Mg calcite (Kamenos *et al.*, 2009) and their ability to change its polymorph (Kamenos *et al.*, 2016). The strength of the Mg-O bond, which is inversely proportional to positional disorder or organization within the crystal lattice, has been linked to a variety of acidification-relative metrics, including pCO_2 of ambient seawater in the cold-water coralline *Lithothamnion glaciale* (Pauly *et al.*, 2015) and aragonite saturation of tropical coral calcifying fluid (DeCarlo *et al.*, 2017).

Here, we investigated the role of acidification-induced changes to the coralline algal skeleton in determining their susceptibility to grazing damage left on the coralline algal surface by limpets and chitons and determine (i) whether grazers preferentially target a particular species, (ii) whether species differ in their skeletal chemistry and (iii) if so, whether grazing intensity and degree of damage has a greater impact on coralline algae with different skeletal chemistries. We also investigated relationships within sample groups to (iv) determine the degree of variability across individuals. Last, we asked (v) if changes in those relationships have occurred under *in situ* ocean acidification over the past 30 years.

Materials and Methods

Specimens

Coralline algal specimens were sampled from Hedophyllum Cove on the NE coast of Tatoosh Island, WA (48.32° N, 127.74° W) during summer months. All sampled specimens were adults of at least 10 years of age, estimated based on specimen size and growth rates (McCoy & Pfister, 2014). Prior to collection, all specimens were transplanted *in situ* onto epoxy putty discs (Sea Goin' Poxy Putty, Permalite Corp.) in areas with natural grazer abundance for >2 years. Collections were made by hammer and chisel, and epoxy discs bearing coralline algal samples were left to dry in the shade and stored dry prior to analysis. Archival *Lithophyllum impressum, Pseudolithophyllum muricatum*, and *Pseudolithophyllum whidbeyense* samples of different individuals from 1981, 1982, 1994, and 1997 were obtained from R.T. Paine and those from 2013 were sampled following Paine's methods.

A Note on Taxonomy

Pseudolithophyllum muricatum, as previously studied on Tatoosh Island, WA (Paine, 1980; 1984; Steneck & Paine, 1986; McCoy, 2013; McCoy & Pfister, 2014; McCoy & Ragazzola, 2014; McCoy *et al.*, 2016), has since been regrouped into the *Crusticorallina* species complex (Hind *et al.*, 2016). A genetic re-characterization of *Pseudolithophyllum whidbeyense* is currently underway (P. Gabrielson, personal communication). We thus refer to these species as *P. muricatum* and *P. whidbeyense* herein to provide consistency with the previous work at this site and to avoid confusion while larger-scale taxonomic relationships are still being clarified. However, we note that *P. muricatum* and *P. whidbeyense* should no longer be interpreted as congeners. We did not study specimens of *Lithothamnion phymatodeum* or articulated *Bossiella* and *Corallina* spp. as those species use physical topography as a grazer defense mechanism.

3D SEM

Uncoated, dry samples were imaged under SEM (FEI Quanta 200F) in low vacuum at both a 0° and 10° stage tilt, using the same physical focal point at the center of each image. These image stereopairs were converted to a 3D image using Alicona MeX 6.1 software (Alicona Imaging). Though samples varied in size, each sample was imaged at ~7 locations to cover its full surface area. Using each composite 3D SEM image, transects were drawn perpendicular to grazing scars to generate a topographical profile of each scar in Alicona MeX. These topographical profiles were saved as image files and using ImageJ (imagej.nih.gov) the width and depth of each grazer mark (identified as a 'valley' feature) were measured and analyzed with reference to the original 3D SEM image to ensure that only true grazer marks were quantified.

Grazing scars are typically made in pairs due to the morphology of molluskan radula. Grazing pressure (defined here as the intensity of grazing) was thus calculated by tallying the number of grazing marks on each SEM micrograph, divided by two and normalized by the area of each imaged area. All SEM micrographs were taken at either 150x or 300x magnification, representing areas of 828750 and 207187.5 μm^2, respectively. Grazing intensity was calculated separately for each 3D SEM image and averaged across the individual specimen.

Raman Spectroscopy

Raman spectroscopy identifies structural molecular fingerprints of materials through a series of vibrational peaks. Raman spectroscopy was conducted using a Renishaw inVia Raman microscope equipped with a LeicaDM2500 M (Leica Microsystems GmbH, Wetzlar, Germany) microscope. Coralline algae were analyzed in epoxy blocks and were excited using a 785 nm

125 laser with a 1200 mm^{-1} grating via a 20x objective. Raman spectra were taken from individual
126 coralline algae adjacent to the areas where grazing was present (identified by 3D SEM). The
127 calcium mineral, full width at half peak maximum (FWHM) and frequency of the peak at ~1089
128 cm^{-1} (v_1) were determined using Renishaw Wire v.3.2 software.
129
130 The v_1 Raman peak (at ~1085-1089 cm^{-1}) identifies as the Mg-O bond from trace Mg present in
131 all natural marine carbonates (Bischoff *et al.*, 1985). The shape of the spectrum is used to
132 differentiate calcite and aragonite (Bischoff *et al.*, 1985), and the Raman shift of the ~1089 cm^{-1}
133 peak is a proxy of Mg content of high Mg calcite (Bischoff *et al.*, 1985; Pauly *et al.*, 2015).
134 Positional disorder of the mineral lattice is caused by shorter and stronger Mg-O bonds, which
135 correspond to smaller FWHM of the ~1089 cm^{-1} peak (Bischoff *et al.*, 1985, Perrin *et al.*, 2016).
136 While Mg concentrations affect FWHM in synthetic carbonates, no consistent relationship has
137 been found in biogenic minerals (Bischoff *et al.*, 1985). To account for this potential effect, we
138 normalized our FWHM data for Mg concentrations by dividing by Raman peak center of the ~v_1
139 peak (*sensu* Pauly *et al.*, 2015). We thus use normalized FWHM to refer to relative mineral
140 organization indicative of changes in positional disorder; higher relative mineral organization
141 (lower positional disorder) is representative of a more robust skeleton (Pauly *et al.*, 2015) . Raw
142 FWHM data is reported in the Supplementary Material. We note there can be a difference in
143 FWHM between biogenic and abiotic carbonates due to difference in the organic load causing
144 difference in symmetrical stretching of C-O bonding. However, this does not apply in our case as
145 we 1) only measured biogenic carbonates (Von Euw *et al.*, 2017), 2) photo-bleached our samples
146 (laser) to remove organic interference, and 3) are using a 785nm laser, which has little sensitivity
147 to organic load.

148

149 *Environmental Datasets*

150 Sea surface temperature (SST) data measured *in situ* every 30 minutes at Hedophyllum Cove on
151 Tatoosh Island, WA are available since 2000. Nearby NOAA buoys measuring SST are located
152 at Neah Bay (NB, No. 46087) and Cape Elizabeth (CE, No. 46041). The NB buoy has been in
153 operation since 2004, and the CE buoy since 1987. While the CE buoy shows a close
154 relationship in SST between Cape Elizabeth and Tatoosh Island (Pfister *et al.*, 2007), it does not
155 extend to 1980 to match our archival sampling. As coastal datasets have been found to be more
156 closely predictive of Tatoosh Island seawater than offshore buoys and satellite data (Pfister *et al.*,
157 2007), we have used monthly averages of the long-term *in situ* temperature record from Race
158 Rocks, BC (48° 17' N, 123° 31' W), which extends back to 1921
159 (http://www.racerocks.com/racerock/abiotic/temperature/seatemperature.htm; Supplemental Fig.
160 S1). As Tatoosh Island SST data did not extend back to the 1980s, a linear regression between
161 SST from Race Rocks, BC and SST from Tatoosh Island, WA was used to determine suitability
162 of using the extended Race Rocks SST record for comparison to skeletal chemistry data from
163 Tatoosh Island. Race Rocks, BC SST was closely correlated to Tatoosh Island, WA, SST (linear
164 regression, r^2=0.297, $F_{1,47}$=21.3, p<0.001; Supplemental Figure S2).

165

166 The Pacific Decadal Oscillation (PDO) index was obtained from NOAA
167 (https://www.esrl.noaa.gov/psd/gcos_wgsp/Timeseries/PDO/; Supplemental Fig. S3, S4). We
168 expect SST and PDO to be highly correlated with each other and other environmental metrics,
169 yet it is unclear which is the most informative (Pfister *et al.*, 2007). We calculated linear
170 relationships between PDO calculated monthly, yearly, monthly minimum, maximum, and SD

by year, and summer (April-July) as well as yearly June-May (the preceding year of growth) and determined that yearly mean PDO was most representative of other metrics, including mean annual SST, except for SD (*sensu* Kroeker *et al.*, 2016; Supplemental Fig. S5, S6). Thus, to rule out the hypothesis of changes in skeletal chemistry resulting from response to SST or PDO, we tested for relationships between Raman metrics of skeletal chemistry and yearly mean and SD of the PDO Index and Raman metrics.

Carbonate chemistry data are available from Tatoosh Island only since 2000 (Wootton *et al.*, 2008; Wootton & Pfister, 2012), thus we do not present correlations between our skeletal chemistry data and carbonate chemistry data. However, isotopic and trace mineral analyses from Tatoosh Island mussel shells reveal abrupt and ongoing changes to the inorganic carbon cycle at this site since the 1970s (Pfister *et al.*, 2011; Bian, 2013). These changes are of a similar magnitude to observed changes in pH in the 2000-2009 period (Pfister *et al.*, 2011), providing evidence for recent changes to the inorganic carbon cycle over the span of our study specimens from 1981-2013.

Statistical Analysis

To determine if grazers target a particular species, we tested grazer mark shape metrics (width, depth) and total grazing pressure by algal species, using a mixed effects model with sample as an interactive random effect (slope and intercept, R package nlme v. 3.1-131) to account for multiple measurements per sample. Within *P. muricatum*, trends in grazer wounds over time were assessed using a 1-way ANOVA, as only one sample was available from each of 1981,

1982, 1994, and 1997, conflating year and individual identity; accordingly, we treat this analysis qualitatively.

To test whether coralline algal species differ in their skeletal chemistry and if chemistry changed over time, we ran a mixed effects model on Raman metrics indicative of Mg content (Raman shift) and relative mineral organization (normalized FWHM) by species and decade. To account for multiple measurements per sample, this was used as an interactive random effect (slope and intercept, R package nlme v. 3.1-131). As both species and decade were significant factors, we tested for effects of decade within each species, again using a mixed effects model with sample as an interactive random effect to better understand these differences.

Relationships between grazer mark shape (depth and width) and skeletal chemistry were assessed using linear regressions. Due to cost and time of SEM analysis, we were not able to study the morphology of grazer marks on historical specimens of *L. impressum* and *P. whidbeyense.* To account for differences in specimen sampling methodology between each analytical technique, we were unable to pair measurement points at the sub-sample level between grazer mark shape and skeletal chemistry. Thus, our smallest unit of variability is the specimen, and we took means and standard deviations by species and decade.

Results

Grazing pressure

Among our samples, all grazer marks were visually identified as molluskan by the parallel lines generated by their radula (Steneck, 1982). No urchin grazing scars were present, which would be shaped in a star pattern generated by the Aristotle's lantern (Steneck *et al.*, 2017). Within

modern 2010s samples, we found no variability in grazing pressure by species ($F_{2,3}$=0.62, p=0.595). In *P. muricatum*, there was no variation in grazing pressure by decade ($F_{1,2}$=0.13, p=0.759).

Grazing wound shape

Grazer mark depth and width varied significantly between algal species in modern 2010s samples (depth, $F_{2,116}$=25.5, p<0.001; width, $F_{2,848}$=77.47, p<0.001). Among these modern samples, *P. muricatum* exhibited the smallest grazer marks and least variation in grazer mark shape by species (Supplemental Table S2). *P. whidbeyense* exhibited the largest grazer marks both in width and depth. Overall, the ratio of grazing wound depth and width is consistent across all specimen types, all marks being much wider than they were deep (Fig. 2c,d). Within modern samples, grazer marks on *P. whidbeyense* were deeper per unit width than those on *L. impressum* and *P. muricatum* (Fig. 2d).

Due to historical sample availability, we analyzed historical specimens for only one individual per calendar year in 1981, 1982, 1994, and 1997. We thus pooled samples by decade (1980s, 1990s, 2010s) to better assess the effect of individual on grazer mark shape trends over time. We analyzed variation in grazer mark depth and width over time on *P. muricatum*, which varied between decades (depth, $F_{1,441}$=38.3, p<0.001; width, $F_{1,441}$=52.3, p<0.001) (Fig. 2a,b). Interestingly, the ratio of width to depth did not differ from historical specimens, though the grazer marks were shallower and less wide on 2010s samples compared to pooled 1980s and 1990s individuals (1-way ANOVA, $F_{1,441}$=56.79, p<0.001).

239 *Skeletal mineralogy*

240 Relative mineral organization (positional disorder), indicated by normalized FWHM, differed by
241 species ($F_{2,51}$=29.9, p<0.001) and decade ($F_{2,8}$=10.8, p=0.006), as did Mg concentrations
242 (species, $F_{2,52}$=14.7, p<0.001; decade, $F_{2,8}$=7.95, p=0.013; Fig. 3). Specifically, each species
243 exhibited a different trend over time, with only *P. whidbeyense* showing a decrease in relative
244 mineral organization over time ($F_{1,19}$=17.7, p<0.001) and no longitudinal trend in either *P.*
245 *muricatum* ($F_{1,19}$=0.008, p=0.93) or *L. impressum* ($F_{1,16}$=0.02, p=0.88; Fig. 3b). The same
246 pattern was observed in each species with regard to Mg concentrations over time, with *P.*
247 *whidbeyense* showing a decline in Raman peak shift ($F_{1,19}$=9.7, p=0.006), and no trend over time
248 in *P. muricatum* ($F_{1,19}$=2.3, p=0.14) or *L. impressum* ($F_{1,16}$=1.8, p=0.20; Fig. 3a). There were no
249 strong relationships between relative mineral organization or Mg concentration and PDO Index
250 (Supplemental Fig. S8), nor between grazer mark width or depth and PDO Index (Supplemental
251 Fig. S9). All Raman spectra were indicative of high-Mg calcite mineral.

252

253 *Relationships between grazing and skeletal chemistry*

254 Mean grazer mark width increased with Mg concentration (slope=7.58, r^2=0.823, p=0.021; Fig.
255 4a). There were no significant relationships between grazer mark morphometrics and Raman
256 metrics of skeletal chemistry on a per specimen basis (Supplemental Fig. S10a, d, g, & j). We
257 measured variability within a sample group (grouped by species and decade) by its standard
258 deviation (SD). Variability in the grazing mark width was strongly correlated with increased Mg
259 concentrations, indicated by increased Raman shift (slope=7.85, r^2=0.987, p<0.001), and with
260 increased mineral organization (slope=1911.8, r^2=0.755, p=0.04; Fig. 4b, c). No additional

relationships were revealed by other pairwise comparisons between individual specimens, sample group means, and sample group SDs (Supplemental Fig. S10).

Discussion

Grazer intensity remained constant over time, and radula marks were proportionally smaller in modern samples (Fig. 2). Grazer intensity was calculated by density of grazing scars on our specimens (Fig. 1) and inferred from field abundance measurements (McCoy & Pfister, 2014). Morphological characteristics of radula marks were used to infer the consistency of grazer identity (Fig. 2). Together, we interpreted these to imply a decline in individual grazer body size, with a maintenance of overall grazing rates by the same grazer type. Indeed, this is corroborated by field abundance measurements of common grazers at the collection site, which showed no trend in grazer abundances over this time period (Fig. 5). *P. whidbeyense* had larger overall grazing scars and had marks with greater depth per unit width than did *L. impressum* and *P. muricatum* (Fig. 2c, Supplemental Table S2). Such differences could be explained by either species-specific grazer preferences (targeting of *P. whidbeyense* by species with differently-shaped teeth) or a difference in skeletal mineralogy that affects grazer wound damage.

Generally across species and decades, we found that grazing wound width was greater at higher skeletal Mg concentration, and more variable either with increasing Mg concentration and relative mineral organization (Fig. 4). Grazing mark size was not related to relative mineral organization, which implies that coralline algae have not become more vulnerable to grazing. This is not what we expected. Decreased mineral organization and an increase in its variability has been observed as a response to high seawater pCO_2 and ocean acidification (Kamenos *et al.*,

2013; Fitzer *et al.*, 2014; Pauly *et al.*, 2015; DeCarlo *et al.*, 2017; McCoy *et al.*, 2018). Given the time series of increasing acidification at our sample site (Wootton *et al.*, 2008; Wootton & Pfister, 2012), we expected a decline in coralline algal skeletal mineral organization or an increase in the variability of mineral organization over time, indicative of poorer control over skeletal deposition. Increased variability of grazer wound width with higher mineral organization can therefore be interpreted as revealing variability of grazing damage based on grazer size and pressure on a structurally sound skeleton or possibly as grazers becoming impacted by ocean acidification before coralline algae.

We note that we did not find a strong correlation between Mg content and mineral organization across any of our samples (Fig. 3c), which corresponds to the results of Bischoff *et al.* (1985), who found an inconsistent relationship between Mg concentration and mineral organization (positional disorder) in biogenic carbonates. While Pauly *et al.* (2015) noted seasonal fluctuations in Mg-O bond strength due to seasonal variation in temperature-linked Mg concentrations, we discount seasonal temperature as a potential driver in this study as all of our samples were collected in early summer across years. Similarly, we did not see a large variation in temperature or PDO across the timescale of our study (Supplemental Fig. S1, S3, S4, S5, S6), nor did we find any significant relationships between PDO and our data (Supplemental Fig. S8, S9). Relative mineral organization (FWHM) and its variability has been found to respond to seawater carbonate saturation states more than to seawater trace element concentrations in aragonite (DeCarlo *et al.*, 2017), potentially offering explanation for the partial decoupling of Mg content and mineral organization in our samples and showing a strong link between ocean acidification and mineralogical structure.

307

308 *P. whidbeyense* was the only species in which skeletal mineralogy changed systematically over
309 time. Unlike our results from pooled specimens, Mg content declined and relative crystal
310 organization decreased in *P. whidbeyense* between the 1980s and 2010s (Fig. 3a,b). The changes
311 observed over time in *P. whidbeyense* skeletal mineralogy are particularly interesting considering
312 recent changes in the ecophysiology of this species. *P. whidbeyense* was historically thinner than
313 both *L. impressum* and *P. muricatum*, however recent acidification stress has reduced all three of
314 these species to that of *P. whidbeyense*'s original thickness (Steneck & Paine, 1986; McCoy &
315 Ragazzola, 2014). Conversely, calcified skeletal inter-filament walls, providing the horizontal
316 partition between cells, have thinned in *P. whidbeyense*, and not in *L. impressum* or *P.*
317 *muricatum* (McCoy & Ragazzola, 2014). These morphology-dependent trade-offs in reducing
318 skeletal volume point to a possible ecophysiological limitation to further thinning (McCoy &
319 Ragazzola, 2014). The ecological niche of *P. whidbeyense* is traditionally that of a relatively
320 poor competitor but fast grower (Paine, 1984), and the reduction of inter-filament wall
321 calcification has been interpreted as a trade-off that preserves its growth rate under acidified
322 conditions (McCoy & Ragazzola, 2014). It seems likely that *P. whidbeyense* may then be more
323 stressed by current seawater conditions than the other species studied here and pressured
324 ecologically to maintain rates of growth and skeletal accretion.

325

326 We suggest that some coralline algae may be increasingly prone to grazing damage as
327 acidification continues in the future. Acidification is also likely to affect grazers of coralline
328 algae concurrent with algal skeletons becoming less resistant to grazing damage. Evidence from
329 other systems suggests increased dissolution of grazing mollusk shells (Hall-Spencer *et al.*, 2008;

Rodolfo-Metalpa *et al.*, 2011), effects on radula, and changes in feeding and metabolic rates (Russell *et al.*, 2013; Leung *et al.*, 2017), all of which will affect grazing pressure through effects on grazer abundance, age-structure, and feeding rates. Acidification effects on non-calcified macroalgae are difficult to generalize across species and environments, but are likely to affect coralline-algal grazers as non-calcified macroalgae compete with coralline algae directly and indirectly through grazer-mediated apparent competition (Cornwall *et al.*, 2011; Hepburn *et al.*, 2011; Celis-Plá *et al.*, 2015; Nunes *et al.*, 2015; Cornwall *et al.*, 2017). Overall, there is mounting evidence that trophic control in marine systems is changing and may potentially play a stabilizing role in the resonance of climate change responses across marine ecosystems (Falkenberg *et al.*, 2013; McCoy & Pfister, 2014; Ghedini *et al.*, 2015; McCoy *et al.*, 2016; Kroeker *et al.*, 2017).

Finally, we note that we observed strong relationships between sample means and standard deviations but not within individual samples. This emphasizes the importance of individual responses to stress and the variety of individual responses within a population (McCoy *et al.*, 2018). Due to the time and cost of analysis, many geochemical studies limit sample replication. We note that in doing so, they may overlook variability due to differential responses between individuals, and may be excluding explanatory mechanisms from their findings that are important to ecophysiological response and interpretation.

Acknowledgements

We are grateful to the Makah Tribal Nation for access to Tatoosh Island and R.T. Paine for making his archival specimens available for analysis. We thank P. Chung for assistance with

SEM imaging, Raman spectroscopy, and training on Alicona MeX 6.1 image processing software. Funding for this research came from a Marine Alliance for Science and Technology Scotland (MASTS) Postdoctoral and Early Career Research Exchange to SJM and NAK. SJM was supported by a Marie Curie International Incoming Fellowship within the 7th European Community Framework Programme (grant agreement FP7-PEOPLE-2012-IIF No. 330271) and by internal funds from Florida State University.

References

Bian N (2013) *Higher resolution minor/trace element and stable isotope study on mussel shells from Tatoosh Island, USA, a coastal upwelling system* (Doctoral dissertation, the University of Chicago, Dept. of Geophysical Sciences). Retrieved from ProQuest Dissertations Publishing (No. 3606296).

Bischoff WD, Sharma SK, MacKenzie FT (1985) Carbonate ion disorder in synthetic and biogenic magnesian calcites: a Raman spectral study. *American Mineralogist*, **70**, 581–589.

Celis-Plá PSM, Hall-Spencer JM, Horta PA, Milazzo M, Korbee N, Cornwall CE, Figueroa FLL (2015) Macroalgal responses to ocean acidification depend on nutrient and light levels. *Frontiers in Marine Science*, **2**, 49–12.

Connell SD, Russell BD (2010) The direct effects of increasing CO_2 and temperature on non-calcifying organisms: increasing the potential for phase shifts in kelp forests. *Proceedings of the Royal Society B: Biological Sciences*, **277**, 1409–1415.

Cornwall CE, Hepburn CD, Pritchard D, Currie KI, McGraw CM, Hunter KA, Hurd CL (2011) Carbon-use strategies in macroalgae: differential responses to lowered pH and implications for ocean acidification. *Journal of Phycology*, **48**, 137–144.

Cornwall CE, Revill AT, Hall-Spencer JM, Milazzo M, Raven JA, Hurd CL (2017) Inorganic carbon physiology underpins macroalgal responses to elevated CO_2. *Scientific Reports*, 1–12.

DeCarlo TM, D Olivo JP, Foster T, Holcomb M, Becker T, McCulloch MT (2017) Coral calcifying fluid aragonite saturation states derived from Raman spectroscopy. *Biogeosciences*, **14**, 5253–5269.

Falkenberg LJ, Russell BD, Connell SD (2013) Future herbivory: the indirect effects of enriched CO2 may rival its direct effects. *Marine Ecology Progress Series*, **492**, 85–95.

Fitzer SC, Cusack M, Phoenix VR, Kamenos NA (2014) Ocean acidification reduces the crystallographic control in juvenile mussel shells. *Journal of Structural Biology*, 1–22.

Ghedini G, Russell BD, Connell SD (2015) Trophic compensation reinforces resistance: herbivory absorbs the increasing effects of multiple disturbances (ed Mouillot D). *Ecology Letters*, **18**, 182–187.

Hall-Spencer JM, Rodolfo-Metalpa R, Martin S et al. (2008) Volcanic carbon dioxide vents show ecosystem effects of ocean acidification. *Nature*, **454**, 96–99.

Hepburn CD, Pritchard DW, Cornwall CE, McLeod RJ, Beardall J, Raven JA, Hurd CL (2011) Diversity of carbon use strategies in a kelp forest community: implications for a high CO2 ocean. *Global Change Biology*, **17**, 2488–2497.

Hind KR, Gabrielson PW, P Jensen C, Martone PT (2016) Crusticorallina gen. nov., a nongeniculate genus in the subfamily Corallinoideae (Corallinales, Rhodophyta) (ed Vis M). *Journal of Phycology*, 1–13.

Kamenos NA, Burdett HL, Aloisio E et al. (2013) Coralline algal structure is more sensitive to rate, rather than the magnitude, of ocean acidification. *Global Change Biology*, **19**, 3621–3628.

Kamenos NA, Cusack M, Huthwelker T, Lagarde P, Scheibling RE (2009) Mg-lattice associations in red coralline algae. *Geochimica et Cosmochimica Acta*, **73**, 1901–1907.

Kamenos NA, Perna G, Gambi MC, Micheli F, Kroeker KJ (2016) Coralline algae in a naturally acidified ecosystem persist by maintaining control of skeletal mineralogy and size. *Proceedings. Biological sciences*, **283**, 20161159–8.

Kroeker KJ, Kordas RL, Harley CDG (2017) Embracing interactions in ocean acidification research: confronting multiple stressor scenarios and context dependence. *Biology Letters*, **13**, 20160802–4.

Kroeker KJ, Sanford E, Rose JM et al. (2016) Interacting environmental mosaics drive geographic variation in mussel performance and predation vulnerability (ed Navarrete S). *Ecology Letters*, **19**, 771–779.

Leung JYS, Russell BD, Connell SD (2017) Mineralogical Plasticity Acts as a Compensatory Mechanism to the Impacts of Ocean Acidification. *Environmental Science & Technology*, **51**, 2652–2659.

McCoy SJ (2013) Morphology of the crustose coralline alga *Pseudolithophyllum muricatum* (Corallinales, Rhodophyta) responds to 30 years of ocean acidification in the Northeast Pacific (ed Hurd C). *Journal of Phycology*, n/a–n/a.

McCoy SJ, Kamenos NA (2015) Coralline algae (Rhodophyta) in a changing world: integrating ecological, physiological, and geochemical responses to global change (ed Gabrielson P). *Journal of Phycology*, **51**, 6–24.

McCoy SJ, Pfister CA (2014) Historical comparisons reveal altered competitive interactions in a guild of crustose coralline algae (ed Jackson S). *Ecology Letters*, **17**, 475–483.

McCoy SJ, Ragazzola F (2014) Skeletal trade-offs in coralline algae in response to ocean acidification. *Nature Climate Change*, **4**, 719–723.

McCoy SJ, Allesina S, Pfister CA (2016) Ocean acidification affects competition for space: projections of community structure using cellular automata. *Proceedings of the Royal Society B: Biological Sciences*, **283**, 20152561–8.

McCoy SJ, Kamenos NA, Chung P, Wootton TJ, Pfister CA (2018) A mineralogical record of ocean change: Decadal and centennial patterns in the California mussel. *Global Change Biology*, **70**, 581–9.

Nunes J, McCoy SJ, Findlay HS et al. (2015) Two intertidal, non-calcifying macroalgae (Palmaria palmataand Saccharina latissima) show complex and variable responses to short-term CO 2acidification. *ICES Journal of Marine Science: Journal du Conseil*, **73**, 887–896.

Paine RT (1980) Food webs: linkage, interaction strength and community infrastructure. *J. Animal Ecology*, **49**, 667–685.

Paine RT (1984) Ecological Determinism in the Competition for Space: The Robert H. MacArthur Award Lecture. *Ecology*, **65**, 1339–1348.

Pauly M, Kamenos NA, Donohue P, LeDrew E (2015) Coralline algal Mg-O bond strength as a marine pCO2 proxy. *Geology*, **43**, 267–270.

Perrin J, Vielzeuf D, Laporte D, Ricolleau A, Rossman GR, Floquet N (2016) Raman characterization of synthetic magnesian calcites. *American Mineralogist*, **101**, 2525–2538.

Pfister CA, McCoy SJ, Wootton JT, Martin PA, Colman AS, Archer D (2011) Rapid Environmental Change over the Past Decade Revealed by Isotopic Analysis of the California Mussel in the Northeast Pacific. *PLoSone*, **6**, e25766.

Pfister CA, Wootton JT, Neufeld CJ (2007) Relative roles of coastal and oceanic processes in determining physical and chemical characteristics of an intensively sampled nearshore system. *Limnol. Oceanogr.*, **52**, 1767–1775.

Ragazzola F, Foster LC, Form A, Anderson PSL, Hansteen TH, Fietzke J (2012) Ocean acidification weakens the structural integrity of coralline algae. *Global Change Biology*, **18**, 2804–2812.

Ragazzola F, Foster LC, Form AU, Büscher J, Hansteen TH, Fietzke J (2013) Phenotypic plasticity of coralline algae in a High CO 2world. *Ecology and Evolution*, n/a–n/a.

Rodolfo-Metalpa R, Houlbrèque F, Tambutté É et al. (2011) Coral and mollusc resistance to ocean acidification adversely affected by warming. *Nature Climate Change*, **1**, 308–312.

Russell BD, Connell SD, Findlay HS, Tait K, Widdicombe S, Mieszkowska N (2013) Ocean acidification and rising temperatures may increase biofilm primary productivity but decrease grazer consumption. *Philosophical Transactions of the Royal Society B: Biological Sciences*, **368**, 20120438–20120438.

Steneck RS (1982) A Limpet-Coralline Alga Association: Adaptations and Defenses Between a Selective Herbivore and its Prey. *Ecology*, **63**, 507–522.

Steneck RS, Paine RT (1986) Ecological and taxonomic studies of shallow-water encrusting Corallinaceae (Rhodophyta) of the boreal northeastern Pacific. *Phycologia*, **25**, 221–240.

Steneck RS, Bellwood DR, Hay ME (2017) Herbivory in the marine realm. *Current Biology*, **27**, R484–R489.

Steneck RS, Hacker SD, Dethier MN (1991) Mechanisms of Competitive Dominance Between Crustose Coralline Algae - an Herbivore-Mediated Competitive Reversal. *Ecology*, **72**, 938–950.

Vergés A, Steinberg PD, Hay ME et al. (2014) The tropicalization of temperate marine ecosystems: climate-mediated changes in herbivory and community phase shifts. *Proceedings of the Royal Society B: Biological Sciences*, **281**, 20140846–20140846.

Von Euw S, Zhang Q, Manichev V et al. (2017) Biological control of aragonite formation in stony corals. *Science*, **356**, 933–938.

Wootton JT, Pfister CA (2012) Carbon System Measurements and Potential Climatic Drivers at a Site of Rapidly Declining Ocean pH (ed Chin W-C). *PLoS ONE*, **7**, e53396.

Wootton JT, Pfister CA, Forester JD (2008) Dynamic patterns and ecological impacts of declining ocean pH in a high-resolution multi-year dataset. *Proc. Natl. Acad. Sci.*, **105**, 18848–18853.

Figure Captions

Figure 1. Grazing pressure in bites $\mu m^{-2}x10^5$ per sample group. *P. muricatum* from the 1980s in light red, 1990s in bright red, and 2010s in maroon. *L. impressum* from the 2010s in blue, and *P. whidbeyense* from the 2010s in green. Species and decade are also labelled on the x-axis. Each point represents grazing pressure observed on an SEM micrograph. Points are jittered for data visualization. Horizontal black lines represent group means and vertical black lines show standard deviation.

Figure 2. A) Grazing mark depth and B) width plotted by specimen type. C) Grazing mark depth over width plotted by specimen type. D) Grazing mark depth plotted versus width (μm), with outliers removed for better visualization. Outliers are included in panels A-C. *P. muricatum* from the 1980s in light red, 1990s in bright red, and 2010s in maroon. *L. impressum* from the 2010s in blue, and *P. whidbeyense* from the 2010s in green. Each point represents an individual grazing mark. Points are jittered for data visualization, and statistics are given in text.

Figure 3. a) Raman shift (cm^{-1}) and b) relative mineral organization, or full width at half maximum (FWHM) normalized to Raman peak center, plotted per species over each sampling time, 1980s, 1990s, and 2010s. c) Normalized FWHM, plotted by Raman shift for each data point. FWHM is plotted x100 and all points are jittered for data visualization. Horizontal black lines represent group means and vertical black lines show standard deviation.

Figure 4. Significant relationships between A) Raman shift (related to Mg concentration) and grazing mark width and B) SD of grazing mark width, and between C) relative mineral organization and SD of grazing mark width. Arrows show direction of increase and interpretation of Raman metrics along each x-axis. *P. muricatum* from the 1980s in light red, 1990s in bright red, and 2010s in maroon. *L. impressum* from the 2010s in blue, and *P. whidbeyense* from the 2010s in green. Linear regressions and statistics given in text. Refer to Supplemental Fig. S10 for plots and statistics of all relationships between specimen mean, sample group mean, and sample group SD.

Figure 5. Grazer abundance over time at Tatoosh Island, WA. Shape indicates different sites around Tatoosh Island, while color denotes grazer species: blue, *Katharina tunicata*; green, *Tonicella lineata*; yellow, *Mopalia ciliata*; pink, *Lottia* spp.; light blue, *Acmea mitra*; and orange, *Strongylocentrotus* spp. Adapted from McCoy and Pfister (2014).

515 Fig 1:

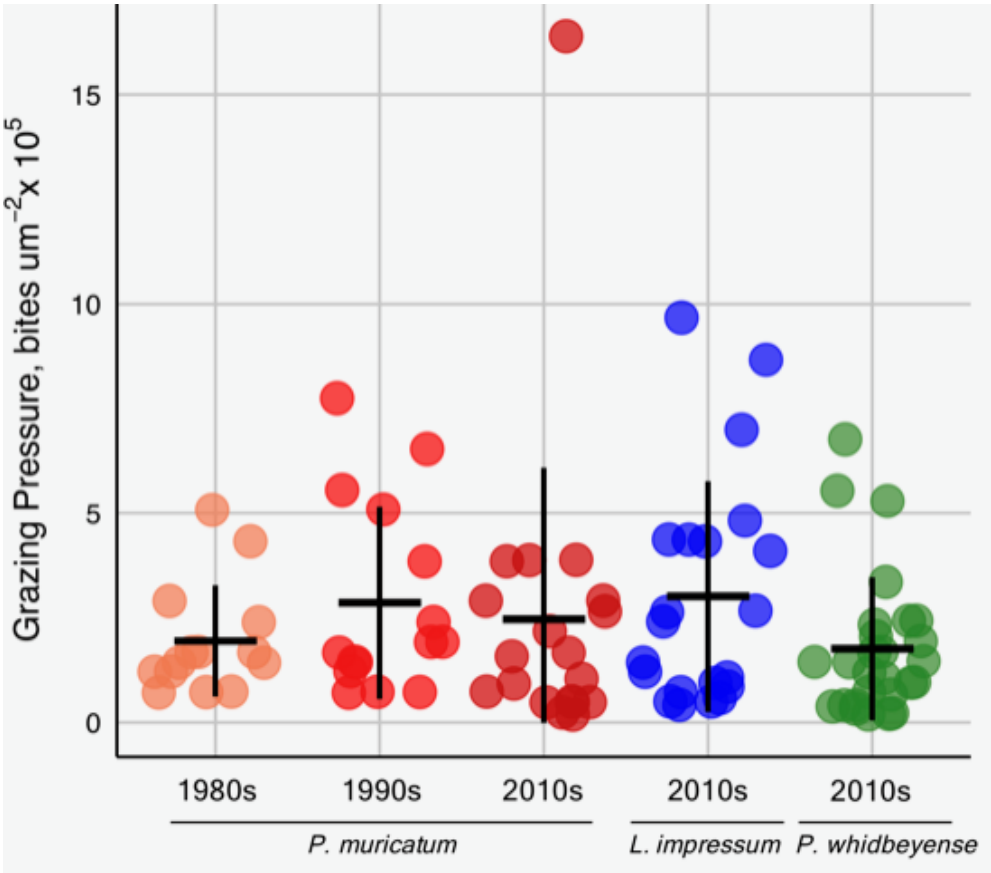

516

517

518

519 Fig 2:

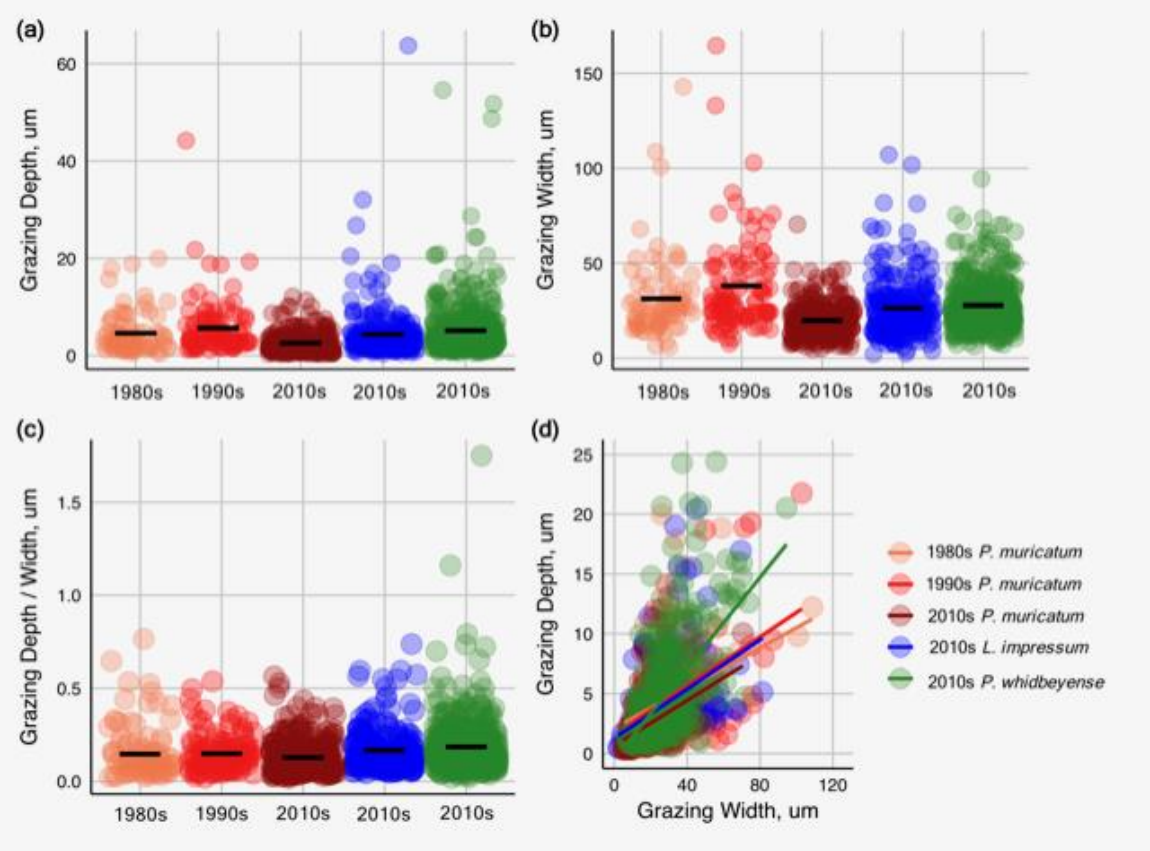

520

521

522

523 Fig 3:

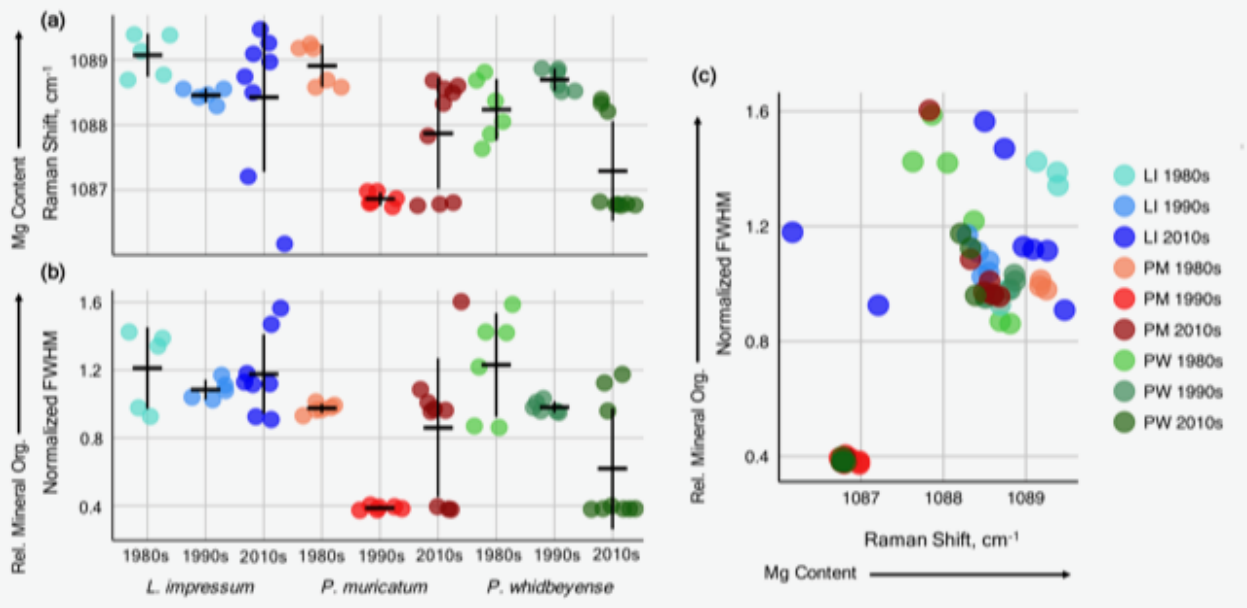

524

525

Fig 4:

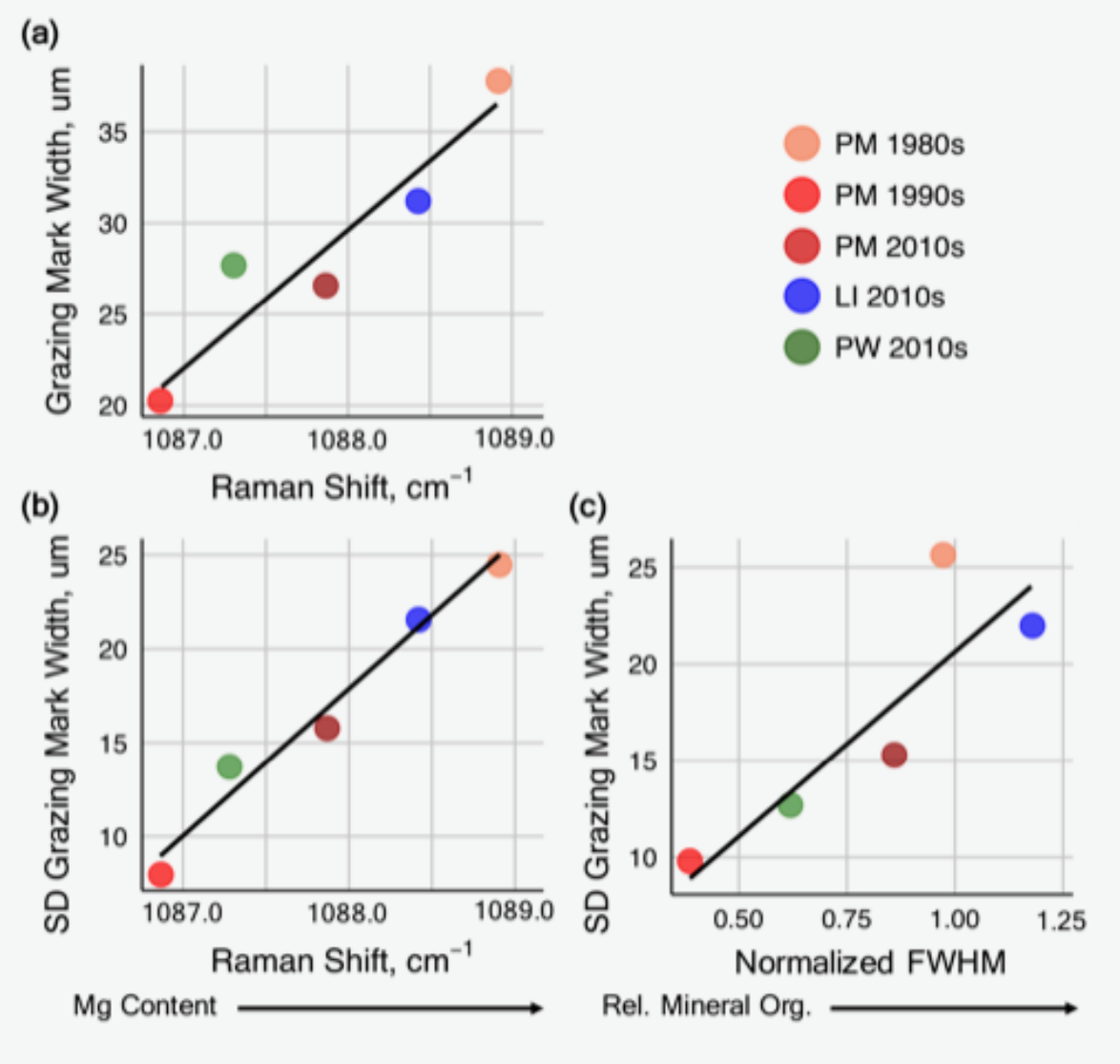
(a)
Grazing Mark Width, um
35
30
25
20
1087.0
1088.0
1089.0
Raman Shift, cm⁻¹
PM 1980s
PM 1990s
PM 2010s
LI 2010s
PW 2010s
(b)
SD Grazing Mark Width, um
25
20
15
10
1087.0
1088.0
1089.0
Raman Shift, cm⁻¹
Mg Content
(c)
SD Grazing Mark Width, um
25
20
15
10
0.50
0.75
1.00
1.25
Normalized FWHM
Rel. Mineral Org.

Fig 5:

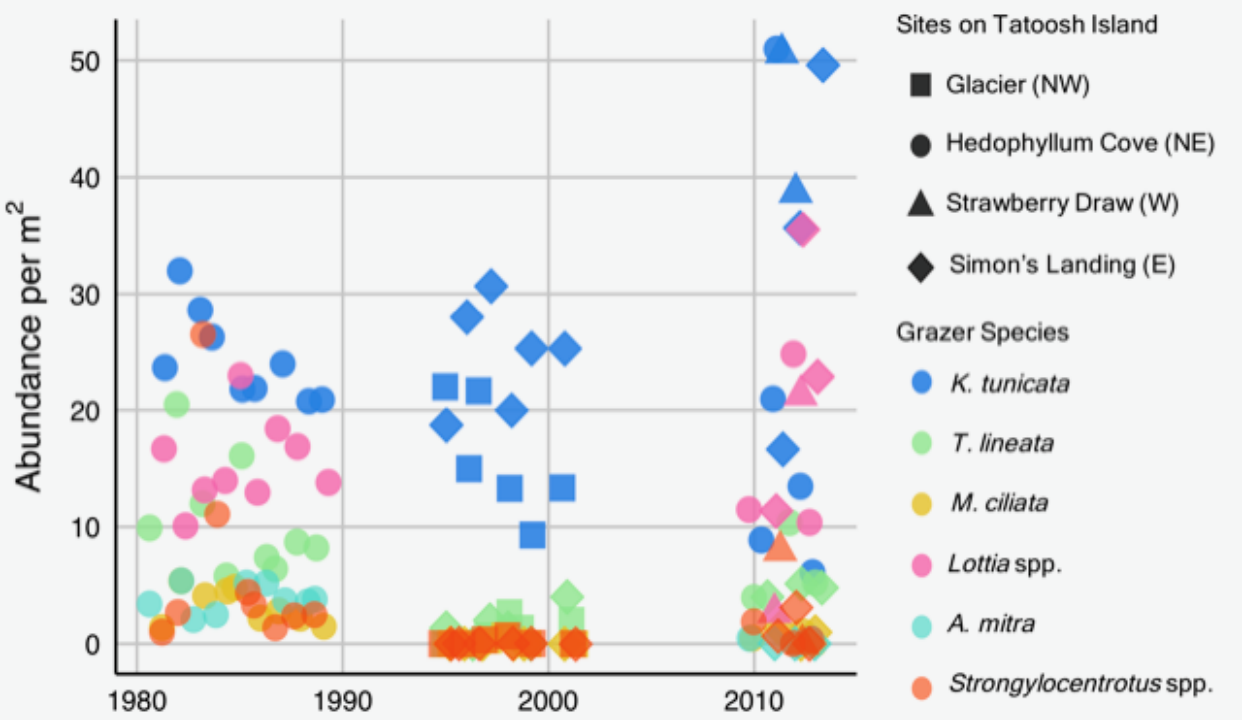
Abundance per m2
50
40
30
20
10
0
1980
1990
2000
2010
Sites on Tatoosh Island
Glacier (NW)
Hedophyllum Cove (NE)
Strawberry Draw (W)
Simon's Landing (E)
Grazer Species
K. tunicata
T. lineata
M. ciliata
Lottia spp.
A. mitra
Strongylocentrotus spp.